Research Article

Rafid Saeed Atea*, Rasha A. Aljazaari and Hasanain M. Dheyab

A case study of T-beams with hybrid section shear characteristics of reactive powder concrete

https://doi.org/10.1515/eng-2022-0424
received January 24, 2023; accepted March 06, 2023

Abstract: As an extension of recent developments in concrete understanding, an extensive study is currently being conducted on the structural performance of reactive powder concrete (RPC). This article guides how to investigate the shear behavior of RPC T-beams and calculate their ultimate and breaking shear capacities. The mechanical features of this construction material and approach to revising the reactive powder shear hybrid segment T-beams are cast-off in this motion and are investigated in this experimental study. To evaluate the effects of volumetric ratio of steel fibers, silica fume ratio, and tensile steel ratio, introductory section on the effectiveness of T-beam shearing reactive powder, the program of experimentation involved trying four beams. The research aimed to determine the deflection conduct of the load, downtime approach, strain amount over the beams' depth, and failure form of cracks. In examining reaction powder's mechanical characteristics mixtures, steel fiber volumetric ratio and silica fume volumetric ratio were also studied. Furthermore, a hybrid beam study revealed that by using reactive powder web and regular concrete in flange effectively, T-beam concert is enhanced when associated with normal concrete T-beams by 12%. Hybrid beams have also revealed that using reactive powder flange and usual concrete in a web effectively advances the show of T-beams when associated with standard concrete T-beams by 28%.

*** Corresponding author: Rafid Saeed Atea,** Civil Engineering Department, Faculty of Engineering, University of Kufa, Najaf, Iraq, e-mail: rafids.aljanaby@uokufa.edu.iq
Rasha A. Aljazaari: Civil Engineering Department, Faculty of Engineering, University of Kufa, Najaf, Iraq, e-mail: rashaa.aljazaari@uokufa.edu.iq
Hasanain M. Dheyab: Civil Engineering Department, Faculty of Engineering, University of Kufa, Najaf, Iraq, e-mail: hasanein.alshammari@uokufa.edu.iq

Keywords: reactive powder, steel fiber, silica fume

1 Introduction

Reactive powder concrete (RPC) is a high-performance cementitious material with imperfect shrinkage and creep, low permeability, ultra-high strength, and amplified corrosion resistance. In 2015, Yoo and Yoon [1] explored the influence of different fibers within the flexural conduct of strengthened UHPFRC beams. A moment's maximum capacity was unaffected by fiber geometry, although lengthy steel fibers pointedly improved post-peak reaction and flexibility. In 2016, Rahman et al. [2] added fibers to plastic concrete to increase its compressive and tensile strengths as well as to control cracking and enhance its durability. All these fibers are used in fiber-reinforced concrete throughout the world. RPC having all the ingredients in powder form is one of the modern types of ultra-high strength concrete where silica fume (SF) is used as pozzolana to achieve high strength. This article focuses on the effect of adding organic fibers (polypropylene) on compressive and tensile strengths of RPC. The organic fibers (polypropylene) produce RPC's compressive and tensile strengths. Furthermore, bending tests of plain RPC samples have been completed and characterized in the form of curves for load–deflection for fiber additions of 0.25–2% (with a 0.25% increment) by weight. In 2018, Alwash and Al-Sultan [3] studied the consequence of two types of fibers (steel fibers and polypropylene fibers) on flexural behavior as well as some important possession (compressive and splitting) assessment of RPC related to normal strength concrete. In 2021, Dawood and Abdullah arranged using different percentages of waste glass powder, steel slag, and SF, compressive and flexural strengths have been tested for such green mortar [4]. In 2022, AL-Shaar et al. presented finite element (FE) modeling using the ABAQUS program to investigate the numerical analysis of high-strength reinforcing steel with conventional strength in reinforced concrete beams under monotonic loading [5].

2 Materials

2.1 Production materials

There is computed normal concrete, and the relevance of a powder that reacts employing disparate preparations preceding the concert of beams in the casting-off products, cement [6], sand, gravel [7], and conventional water is processed without any additions. Also SF [8] and steel [10] fibers are cast-off for reactive powder concrete for RPC T-beams.

2.2 SF

Table 1 displays the chemical forms of SF cast-off in this exploration. SF meets the requirements [8].

2.3 Superplasticizer (SP)

Glenium 51 is a fantastic effective concrete SP employed in this amendment [9] (Table 2).

2.4 Steel fibers

Steel fibers with high performance were utilized in the study [10], and their attributes are listed in Table 3.

2.5 Steel reinforcement

Three 1,000 mm long specimens, each with insignificant diameter, are put on trial to determine the stress on middling yield f_y and ultimate toughness f_u [11] (Table 4).

Table 1: Chemical characteristics of SF

Oxide composition	Abbreviation	Oxide satisfied (%)	Maximum requirement for conditions
Silica	SiO_2	94.87	85.0 (min)
Alumina	Al_2O_3	1.18	–
Iron oxide	Fe_2O_3	0.09	–
Lime	CaO	0.23	–
Magnesia	MgO	0.02	–
Sulfate	SO_3	0.25	–
Oxygenated potassium	K_2O	0.48	–
Ignition injury	L.O.I.	2.88	6.0 (max)
Moisture level	–	0.48	3.0 (max)

Table 2: Properties of SP

Method	Viscous liquid
Marketable name	Glenium 51
Chemical composition	Naphthalene formaldehyde condensates
Secondary impact	Improvement in early and final compressive strength
Color	Light brown
Comparative density	1.1 g/cm^3 at 20°C
pH	6.6
Viscosity	128 ± 30 cps @ 20°C
Transference	Not considered to be dangerous
Labeling	No hazard label obligatory
Chloride satisfied	None

3 Mixing concrete

In this study, two types of concrete compositions were discarded.

3.1 Typical concrete mixture

Cement, fine aggregate, coarse aggregate, and water were all thrown away in a conventional concrete composition, including molding the ordinary and web in hybrid beams. RPC1, RPC2, and RPC3 (normal, RPC1, RPC2, and RPC3).

3.2 Concrete mixes with reactive powders

The quantities of materials of all mixtures are given in Tables 5 and 6 (Figure 1).

3.3 Mechanical properties of RPC

All the observations are shown in Table 7.

Table 3: Steel fiber characteristics

Configuration	Property	Specification
	Description	Hooked
	Length	30 mm
	Diameter	0.375 mm
	Density	7,800 kg/m^3
	Tensile strength	1,800 MPa
	Modulus of elasticity	200 GPa
	Aspect ratio (L_f/D_f)	80

Table 4: Steel bars' characteristics

Minor diameter (mm)	Real diameter (mm)	f_y (MPa)	f_u (MPa)	Extension (%)
10	10.06	490	635	11
12	12.05	458	643	12
20	20.11	580	680	14

3.4 Load–mid-span deflection according to concrete type (hybrid section)

Normal, RPC1, RPC2, and RPC3 load–mid-span deflections are confirmed in Figure 2.

3.5 Inclined crack width

A fracture detection pocket microscope was cast-off to portion the major crack in the beam. Figure 3 shows the

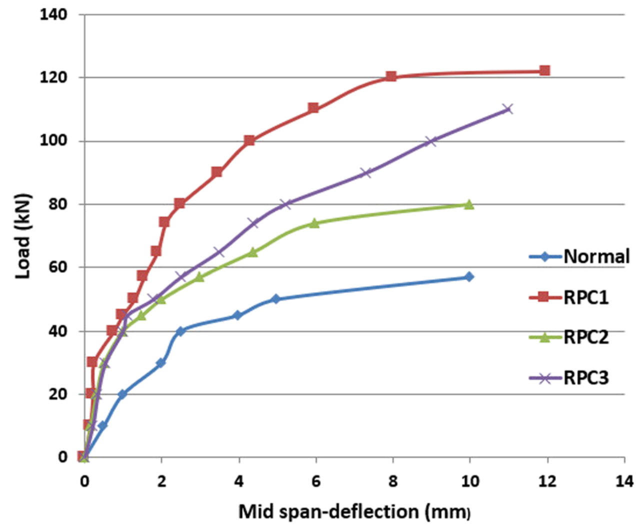

Figure 2: Hybrid section's effects on mid-span deflection curves of T-beams.

Table 5: Characteristics of various RPC mix types

Combination♣	Cement (kg/m^3)	Sand (kg/m^3)	SF* (%)	SF (kg/m^3)	w/cementitious	SP** (%)	Steel fiber*** (%)	Steel fiber (kg/m^3)
M0,25	1,000	1,000	25	250	0.2	1.7	0	0
M1,25	1,000	1,000	25	250	0.2	1.7	1	78
M2,25	1,000	1,000	25	250	0.2	1.7	2	156
M2,20	1,000	1,000	20	200	0.2	1.7	2	156
M2,15	1,000	1,000	15	150	0.2	1.7	2	156

♣ The letter M denotes mix no. *SF weight as the total cement weight. ** SP, percent of binder weight. ***Ratio of total mixture volume.

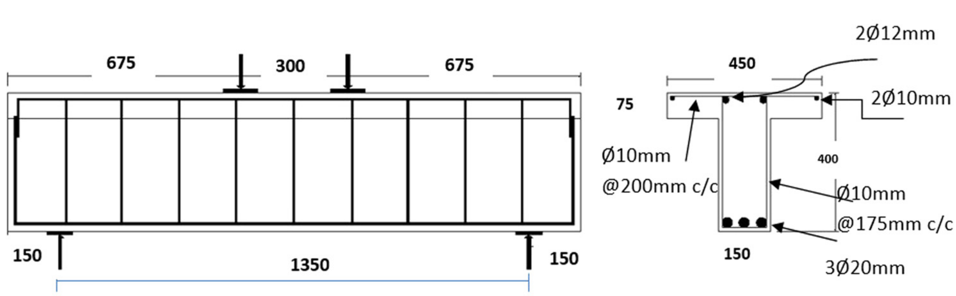

Figure 1: Cross-sectional and dimension details and beam reinforcement (normal, RPC1, RPC2, and RPC3). *All dimensions in (mm).

Table 6: Beam details and concrete properties

Group no.	Parameter	Beam	V_f (%)	SF (%)	Tensile reinf.	Concrete in section
1	Changing concrete in section	N.C.	–	–	2ϕ12	Normal in all section
		RPC1	2	25	2ϕ12	RPC in all section
		RPC2	2	25	2ϕ12	RPC only in the flange
		RPC3	2	25	2ϕ12	RPC only on the web

Table 7: Results of mechanical properties of hardened concrete tests

No. of mix	Mix type	Steel fiber V_f (%)	SF (%)	f'_c* (MPa) [12]	f_t** (MPa) [13]	f_r*** (MPa) [14]	E_c**** (MPa) [15]
1	M0,25	0	25	74.62	5.49	5.29	40,611
2	M1,25	1	25	78.43	5.63	5.48	41,711
3	M2,25	2	25	88.27	6.176	5.82	44,213
4	M2,20	2	20	83.45	5.89	5.67	42,794
5	M2,15	2	15	80.23	5.79	5.57	42,113
6	M_{normal}	–	–	27.84	3.054	3.19	24,531

*f'_c(MPa): strength in compression. **f_t (MPa): splitting tensile capability. ***f_r (MPa): rupture modulus. ****E_c (MPa): elastic modulus.

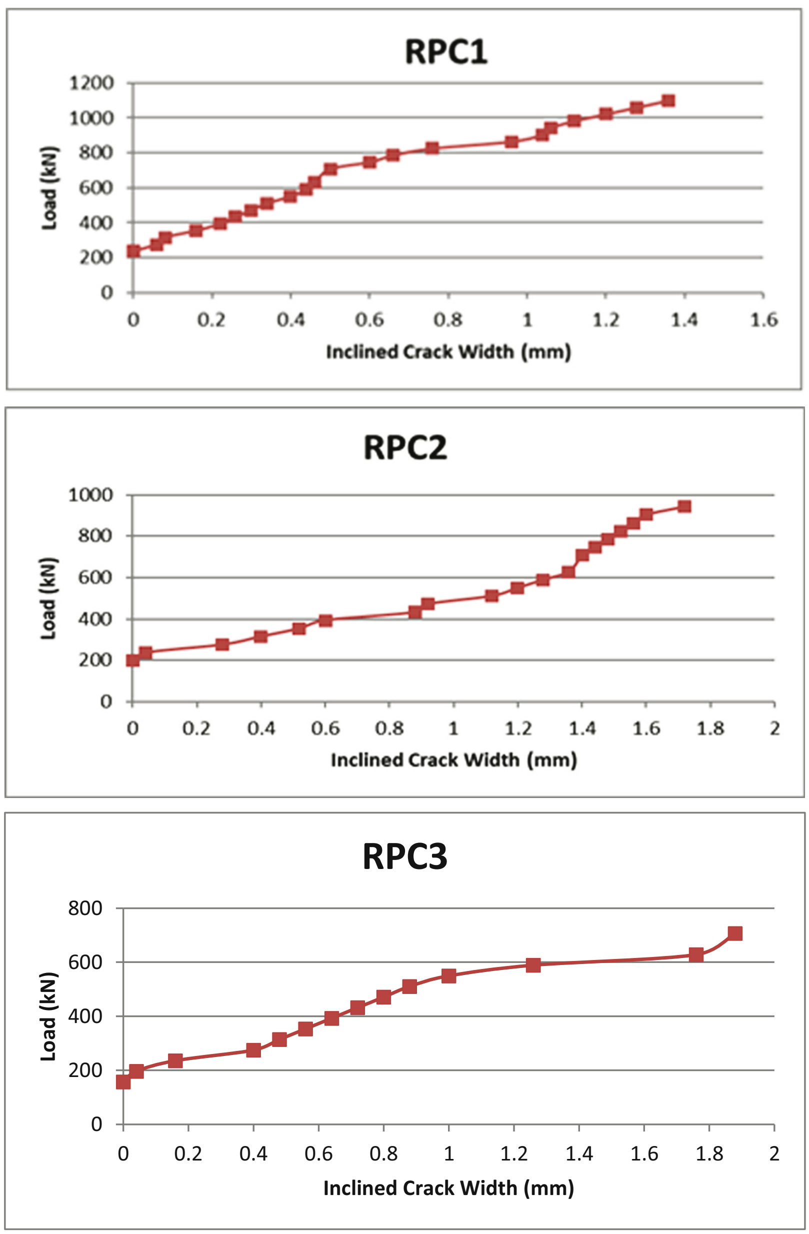

Figure 3: Width of a load-inclined crack.

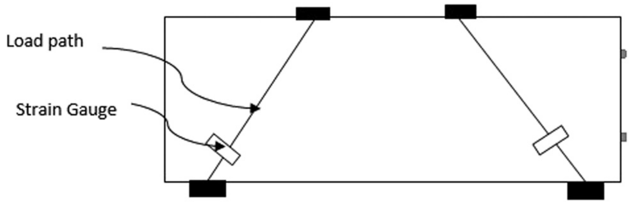

Figure 4: Location of strain gauge.

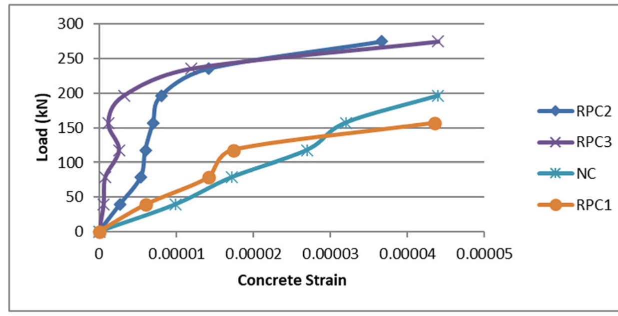

Figure 5: Load–concrete strain (by electrical strain gauges).

relation between loads and crack width. From this figure, it is clear that beams through a higher *a*/*d* ratio at an equal load level showed higher crack width. It is also observed

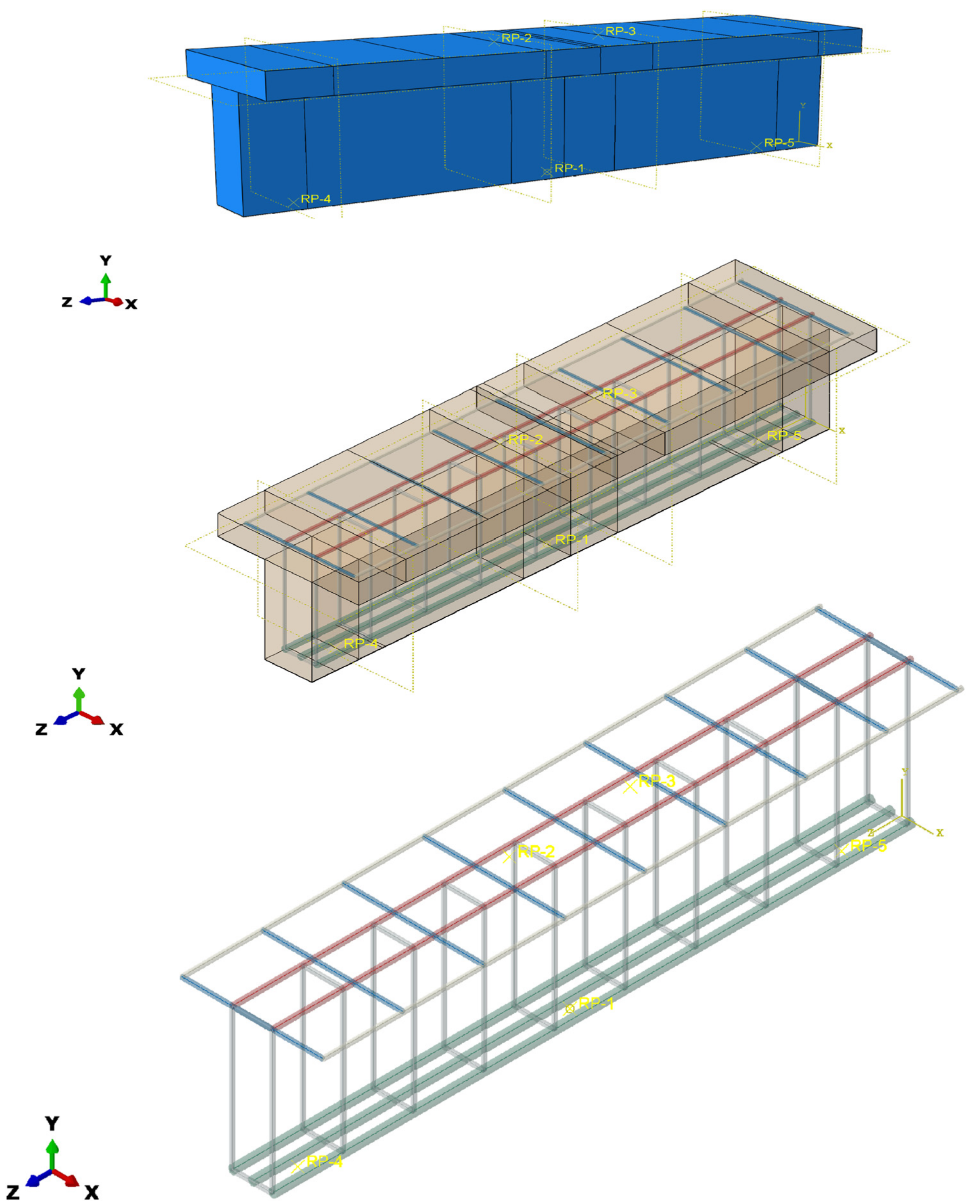

Figure 6: Modeling of cross-sectional and reinforcement for T-beam.

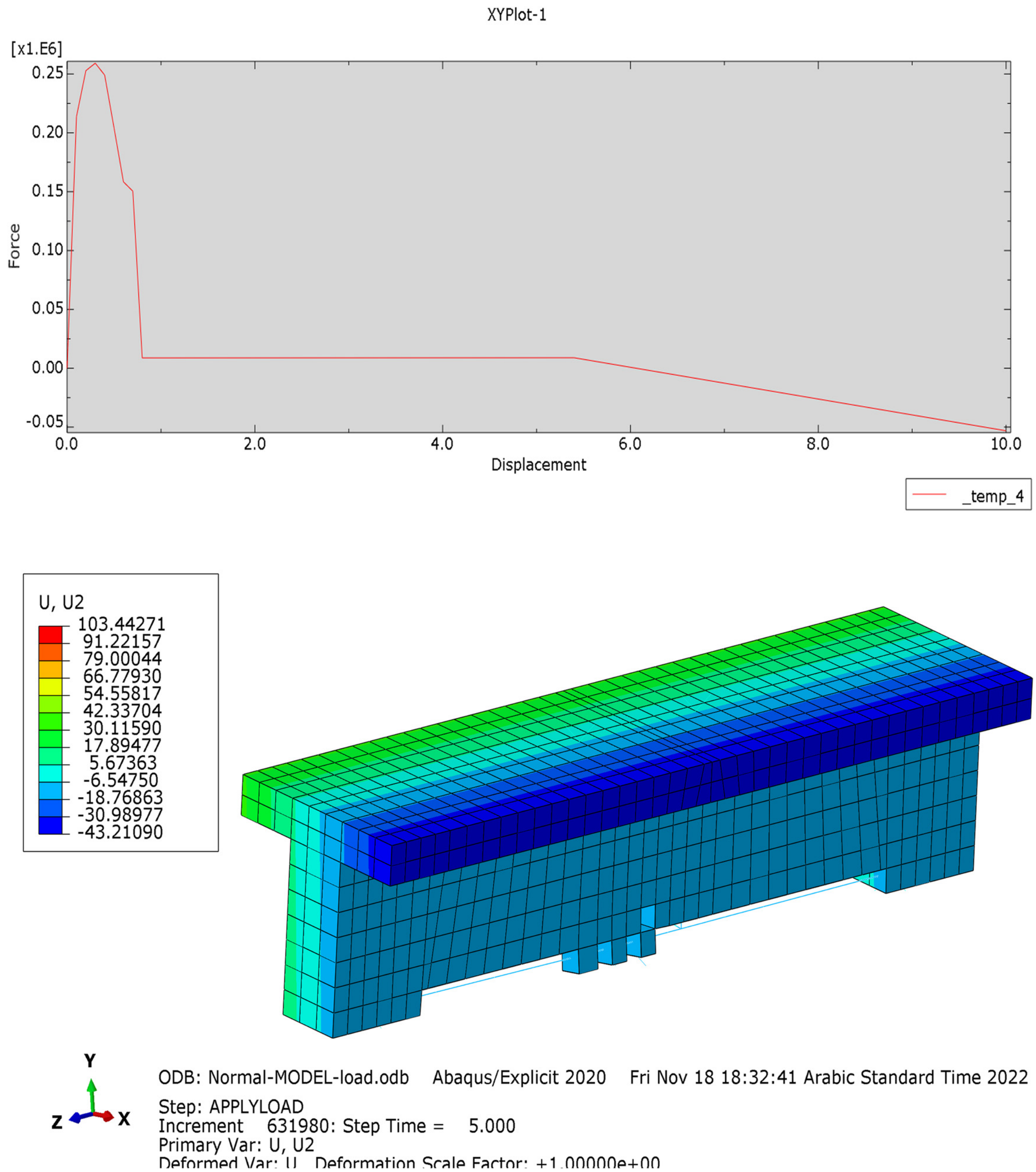

Figure 7: Displacement for mid-specimen N.C.

that figure beams with web reinforcement have a smaller crack width than those without web reinforcement. But at the load step just before failure, beams with web reinforcement showed higher crack width, and the failure did not occur suddenly.

3.6 Distribution of strains

The concrete strains in the middle of the spectrum part of the confirmed beams were unhurried on seven different points, as shown in numbers. Figure 4 depicts the location where the strain was measured for each beam. In Figure 5, for all beams, the tensile strain at the load path's middle length was measured.

4 Numerical element work

To analyze the beams, FEs are obsolete; the ABAQUS application provides choices for describing several types of material behavior; eight-node isoparametric brick pieces

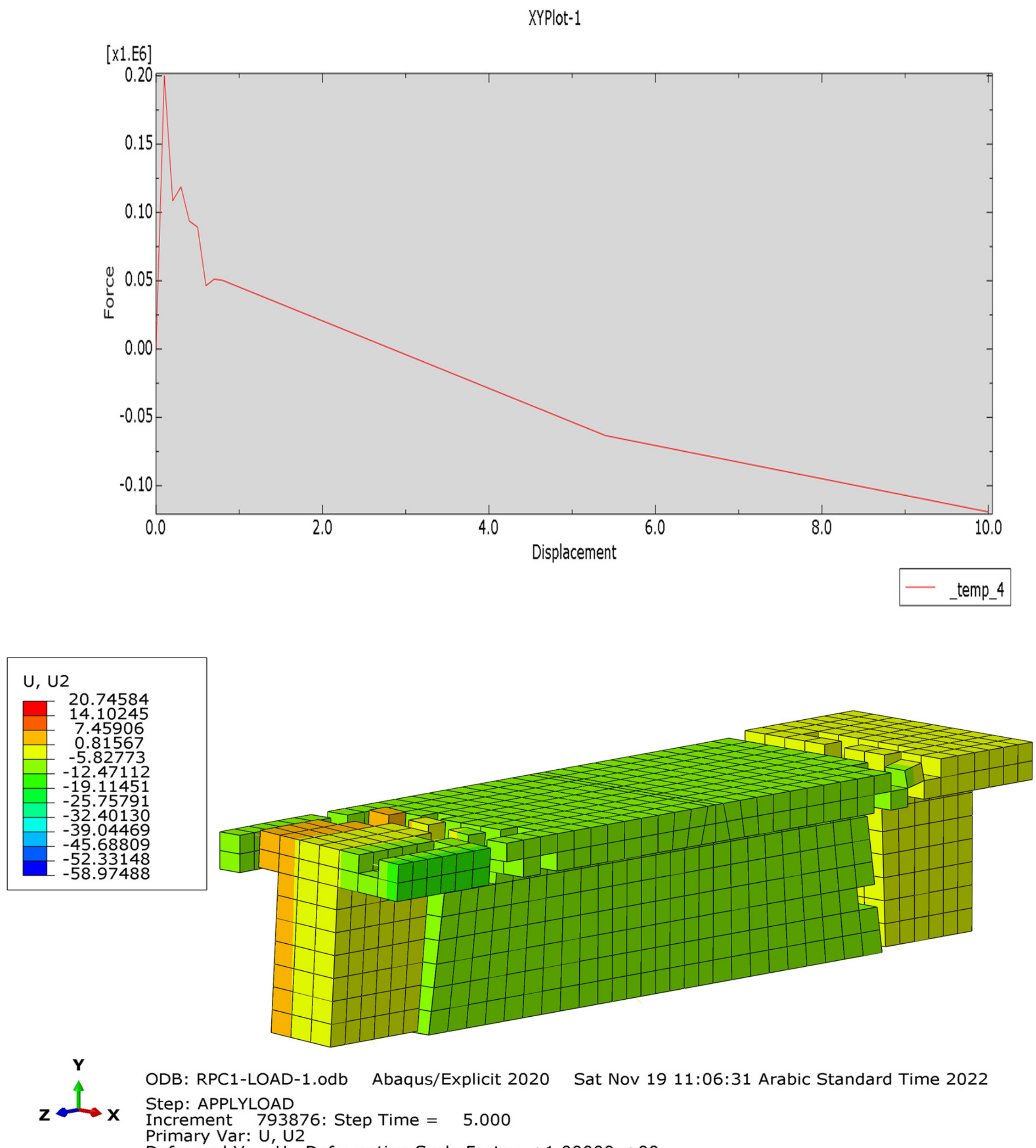

Figure 8: Displacement for mid-specimen RPC1.

represent concrete. Employing four-node link components for steel reinforcement [16]. Figure 6 contains all details.

4.1 FE results

4.1.1 Displacement for specimens

Figures 7–10 express that the investigative data and computational load for these species' center beam deflection for direction *Y* are arranged correctly.

4.1.2 Concrete strain distribution

Figures 11–13 express the numerical concrete plastic-strain distribution of beams and damage. It can be seen from these figures that the largest strain occurred along the load path where the tending fracture occurred. Additionally, it showed that the position where the largest rate of strain followed was slightly below the midpoint of the load path, which corresponds to the location where the maximum crack width was confirmed in the exploratory study (Figure 14).

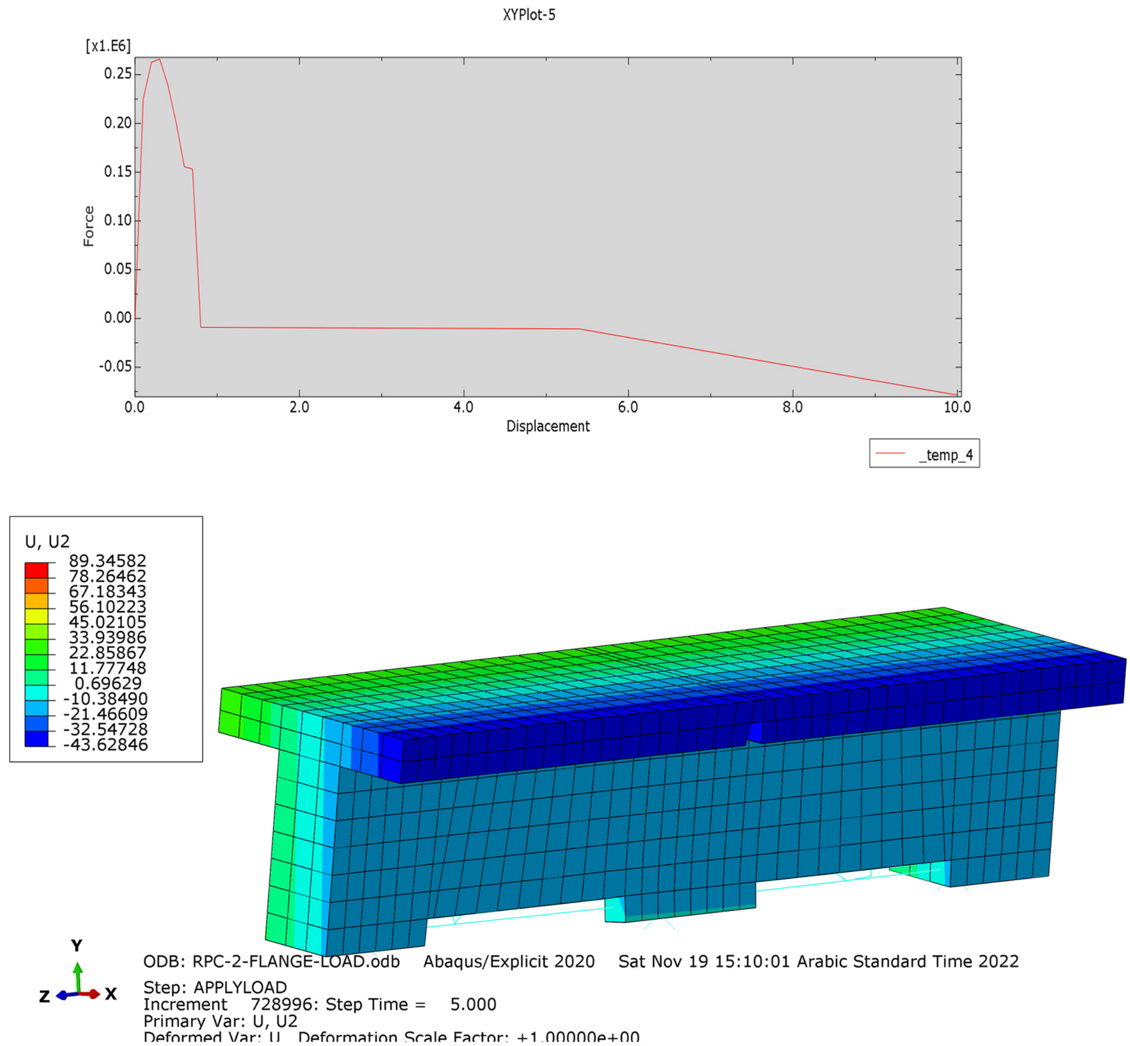

Figure 9: Displacement for mid-specimen RPC2.

5 Conclusions of the experimental work

1. The insertion of steel fibers significantly improves the strength in compression (f_c') of RPC according to the results. When fibers are present in portions of volume of 0.5, 1.0, 1.5, and 2.0%, the compressive strength is increased by 20, 25.6, 32, and 41%, respectively, over fibro-free RPC. The impact of steel strands' tensile strength at splitting and rupture modulus is still greater. Over the nonfibrous RPC, the tensile strength of the splitting was improved by 67.3, 100, 163.6, and 180%, respectively, while the modulus of rupture increased by 75.4, 110.5, 164, and 233.3% with the rise in fiber volume by the same amount.
2. Although the number of steel fibers in the RPC combination had no consequence on the primary diagonal cracking stress, it does impact the ultimate load. The diagonal cracking load increases by 20.0, 20.0, 30.0, and 40.0% when the fibers' volume proportion increases from 0 to 0.5, 1.0, 1.5, and 2.0, respectively, and is associated with nonfibrous RPC beam. In addition, with the equivalent rise in fiber volume percentage, the final strength in shear of nonfibrous RPC specimens also increases by 87.3, 97.2, 118.3, and 132.4%, respectively.
3. When the SF content is the same amount diagonal cracking load is raised by 7.14 the RPC beams are increased from 5 to 10, 15, and 21.4%, respectively, while the total load rises by 6.06 and 9.09%.
4. Curves of load deflection for steel-fiber beams (0, 1, and 2%), an expression that as the steel fiber volumetric ratio rises, the deflection reduces at a given load level at all loading steps due to an upsurge in stiffness.

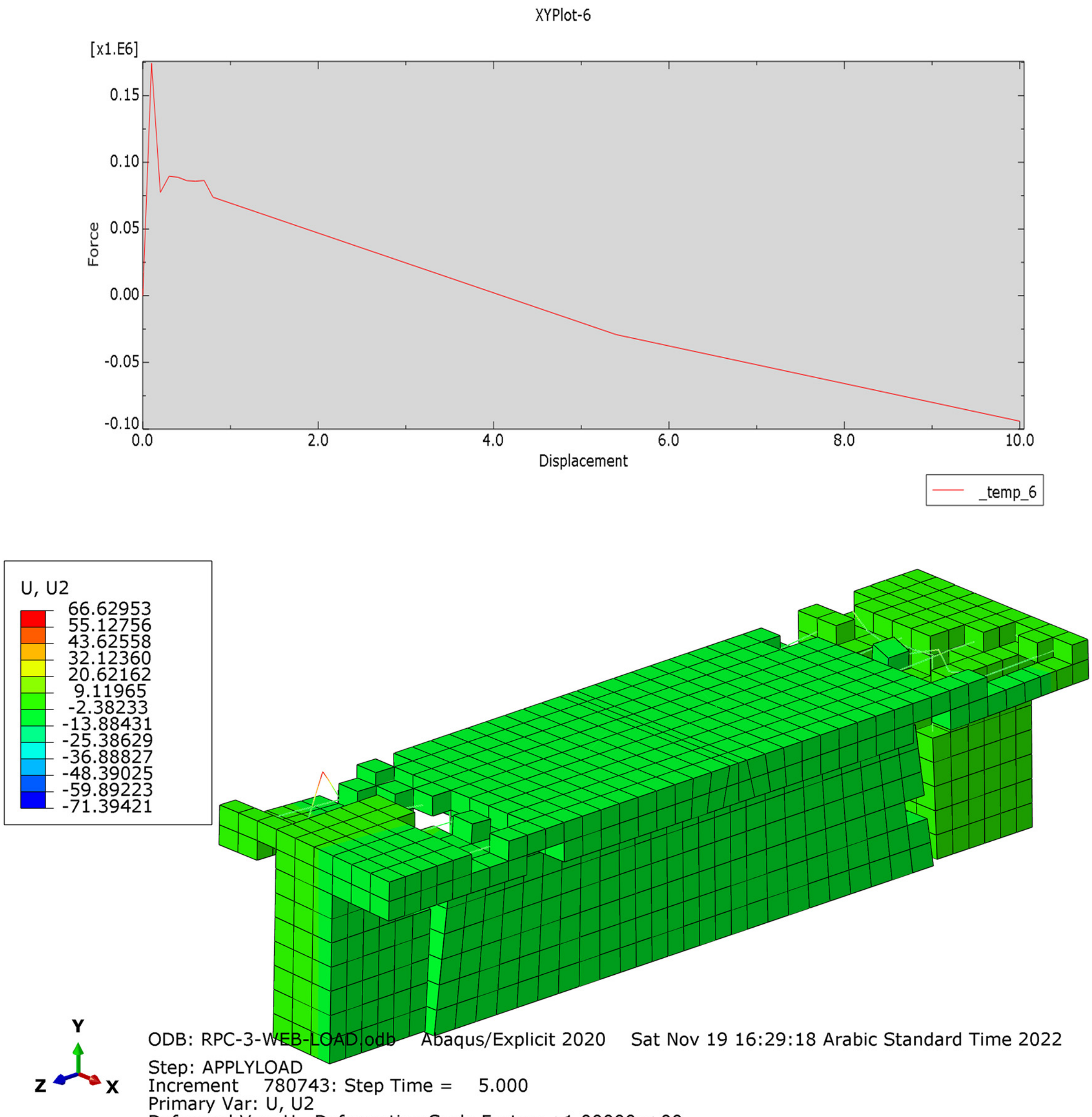

Figure 10: Displacement for mid-specimen RPC3.

5. SF in concentrations ranging from 15 to 25% does not affect the major fracture capacity, ultimate shear, or RPC T-beams deflection in the middle of its span. The major fracture load, ultimate deflection of the mid-span, and shear strength, on the other hand, grow from 15 to 25% with percentages of 17, 10, and 15%, respectively.
6. RPC cylinders tested in compression had a peak strain of 0.0025. Peak strain was increased by 44, 60, 72, and 92% when portions of volume at 0.5, 1.0, 1.5, and 2.0% of steel fibers were added, resulting in 0.0036, 0.0040, 0.0043, and 0.0048, respectively.
7. The displacement curves and strain distribution figures used to describe the behavior of the FE models generally exhibit high agreement with the corresponding experimental curves.

Conflict of interest: The authors state no conflict of interest.

Data availability statement: Most datasets generated and analyzed in this study are comprised in this submitted manuscript. The other datasets are available on reasonable request from the corresponding author with the attached information.

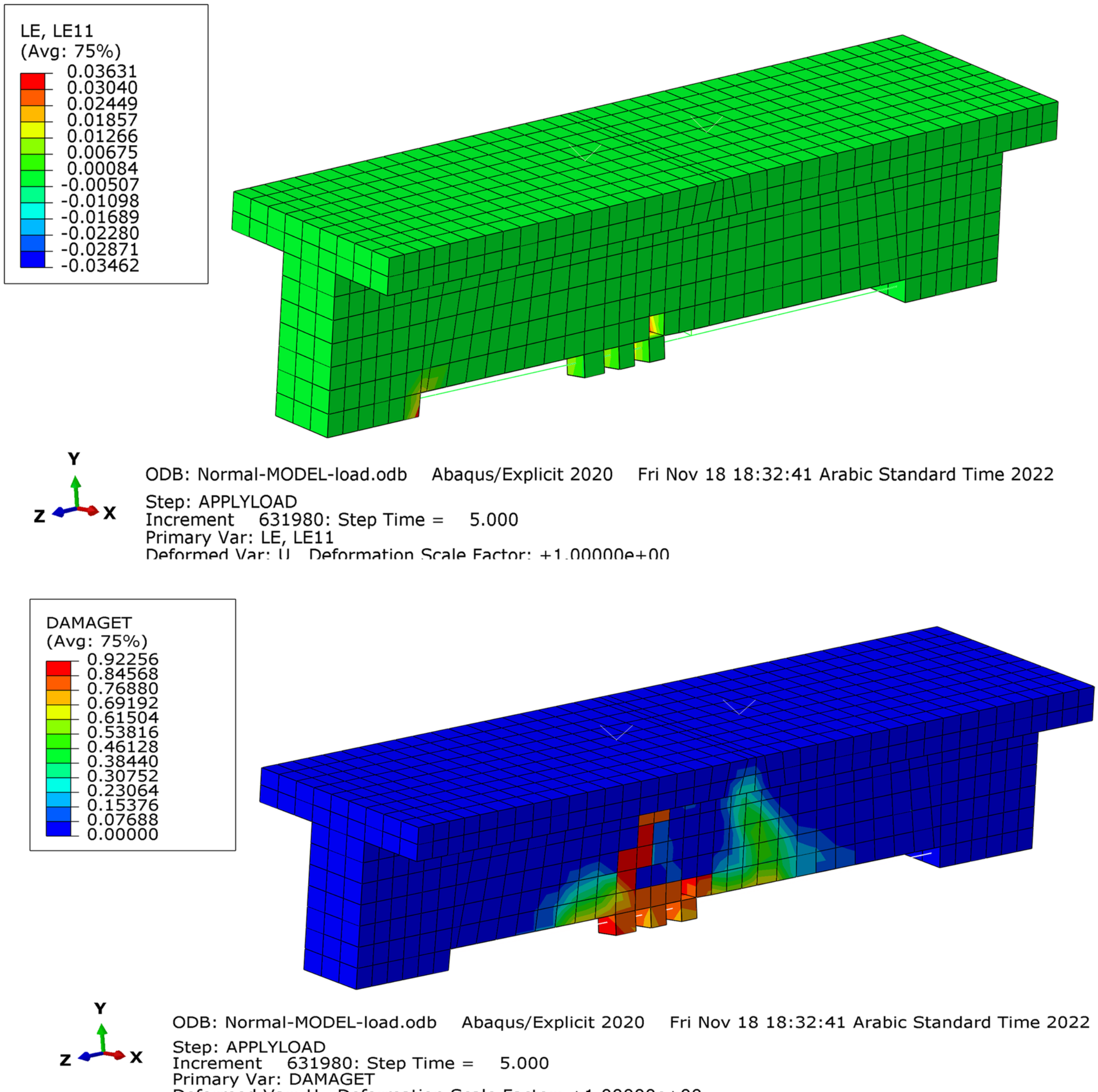

Figure 11: Analysis of strain variation and damage in specimen N.C.

References

[1] Yoo DY, Yoon YS. Structural performance of ultra-high concrete beams with different steel fibers. Eng Struct. 2015;102:409–23.

[2] Rahman Z, Naseer A, Adil M. Effect of polypropylene-fibers on compressive and tensile strengths of reactive powder concrete. ARPN J Sci Technol. 2016;6(2):34–7.

[3] Alwash JJ, Al-Sultan SM. Flexural behavior of reactive powder concrete beams with various types of fibers. Int J Civ Eng Technol. 2018;9(4):32–44. http://iaeme.com/Home/issue/IJCIET?Volume=9&Issue=4.

[4] Dawood ET, Abdullah MH. The behavior of non-reinforced green mortar with fibers has been observed. Open Eng. 2021;11:67–84. doi: 10.1515/eng-2021-0006.

[5] Harba IS, Abdulridha AJ, AL-Shaar AA. Numerical analysis of high-strength reinforcing steel with conventional strength in reinforced concrete beams under monotonic loading. Open Eng. 2022;12:817–33. doi: 10.1515/eng-2022-0365.

[6] Iraqi Standards No.5/1984. Ordinary Portland cement. Ministry of Housing and Construction, Baghdad; 2004.

[7] Iraqi Standards No.45/1984. Aggregate from natural sources for concrete and construction. Ministry of Housing and Construction, Baghdad; 2004.

[8] ASTM C1240-04. Standard Specification for the Use of Silica Fume as a Mineral Admixture in Hydraulic Cement Concrete, Mortar and Grout. Vol. 4.2; 2004. p. 6.

[9] ASTM C494/C494M-1999a. Stand Specif Chem Admix Concr. Vol. 01.02; 1999.

[10] ASTM A 820/A 820M-04. Standard Specification for Steel Fiber for Fiber-Reinforced Concrete; 2004. p. 1–4.

[11] ASTM A615/615M-05a. Standard Specification for Deformed and Plain Carbon Structural Steel Bars for Concrete Reinforcement. Annual Book of ASTM Standards. Vol. 01.02; 2005.

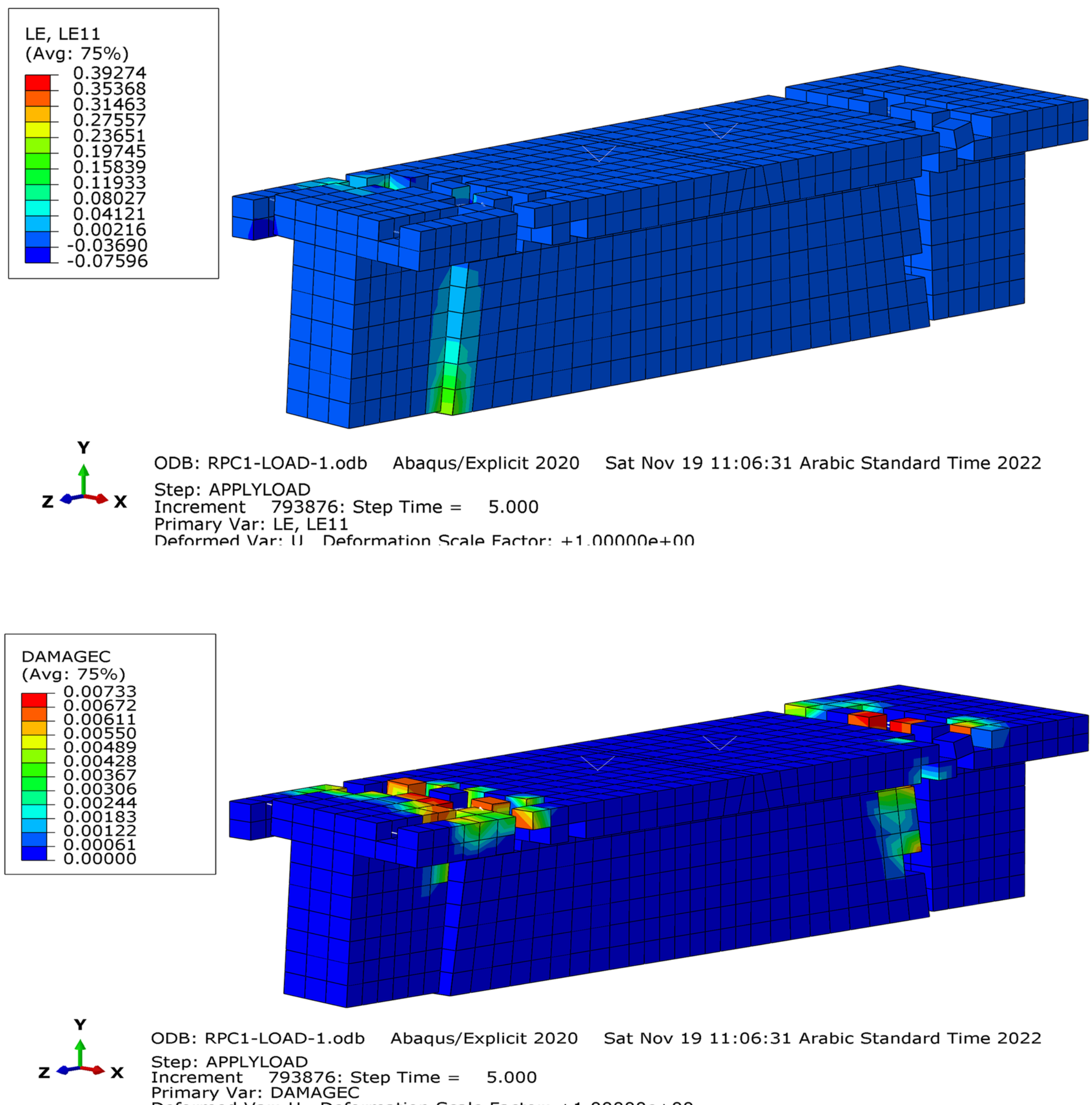

Figure 12: Analysis of strain variation and damage in specimen RPC1.

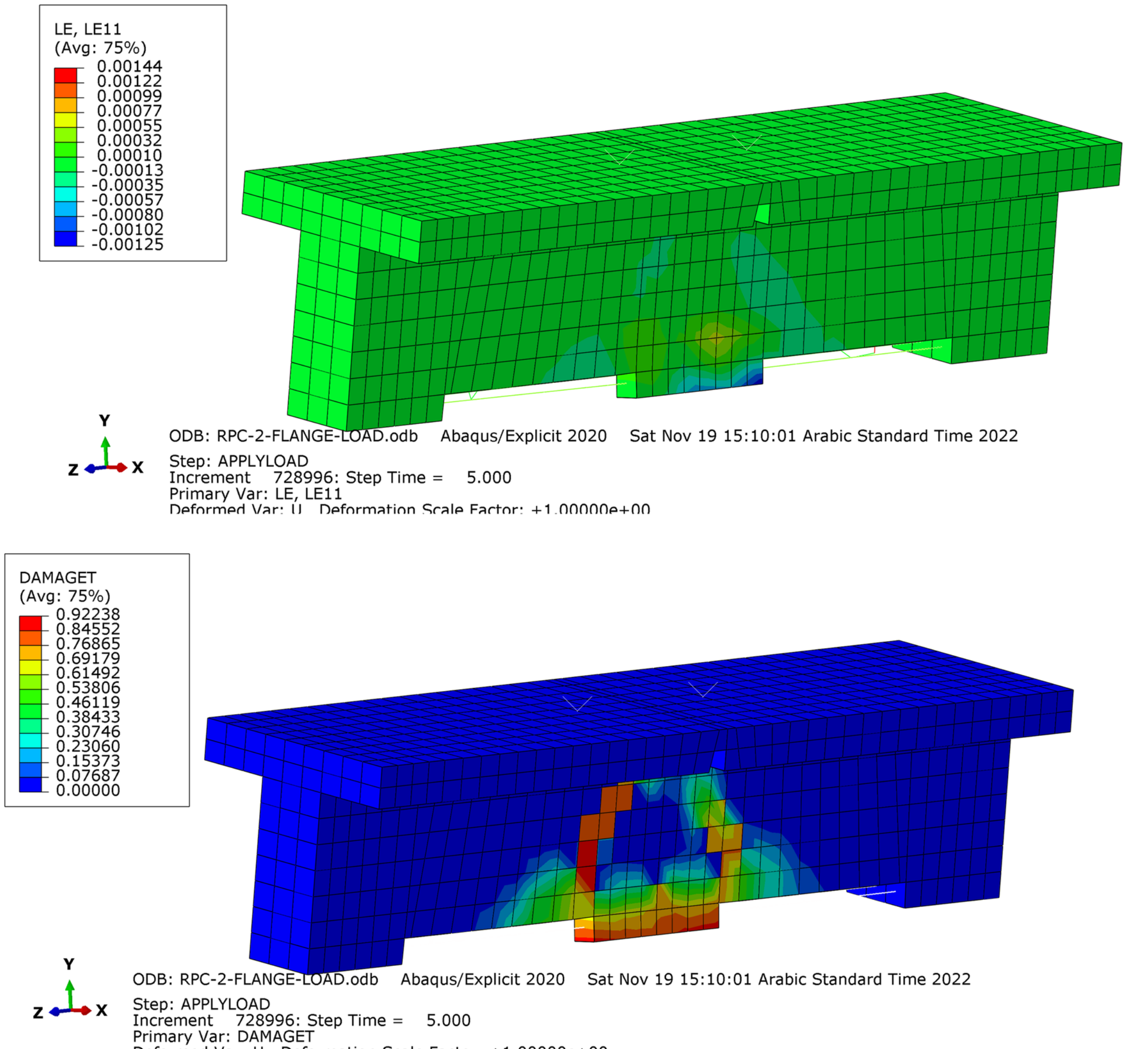

Figure 13: Analysis of strain variation and damage in specimen RPC2.

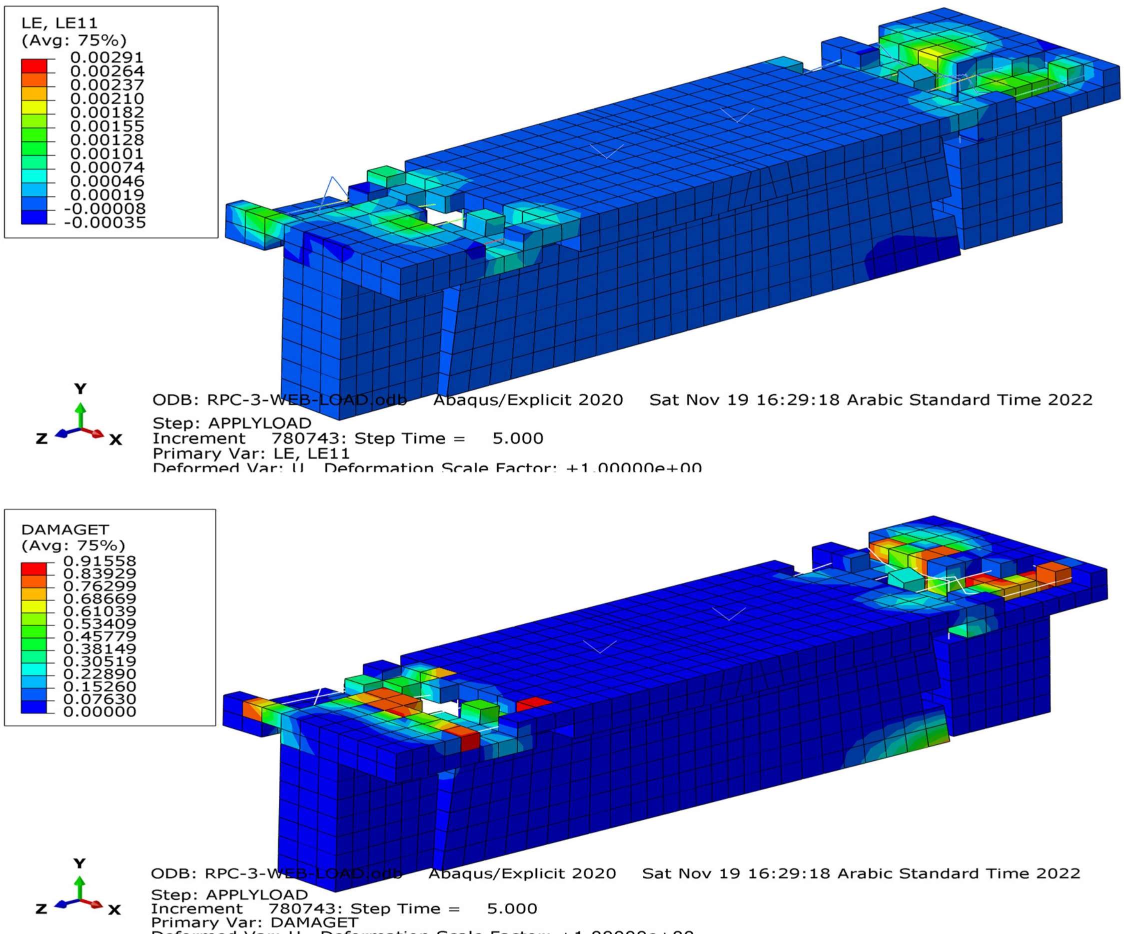

Figure 14: Analysis of strain variation and damage in specimen RPC3.

[12] ASTM C39/C39M-2003. “Standard Test Method for Compressive Strength of Cylindrical Concrete Specimens”, Vol. 4.2, 2003, pp. 1–5 and B.S. 1881: Part 116: 1983, "Methods for Determination of Compressive Strength of Concrete Cubes", January 1983, pp. 1–8.

[13] ASTM C78-02. Standard Test Method for Flexural Strength of Concrete (Using Simple Beam with Third-point Loading). Vol. 4.2; 2002. p. 1–3.

[14] ASTM C496/C496M-04. Standard Test Method for Splitting Tensile Strength of Cylindrical Concrete Specimens; 2004; Vol. 4.2. p. 1–5.

[15] ASTM C469-02. Standard Test Method for Static Modulus of Elasticity and Poisson’s Ratio of Concrete in Compression. Vol. 4.2; 2002. p. 1–5.

[16] ACI 318M-11. Building Code Requirements for Structure Concrete and Commentary. American Concrete Institute; 2011.